



Published in final edited form as:

Environ Sci Technol. 2011 October 1; 45(19): 8559–8566. doi:10.1021/es201309c.

Environmentally Persistent Free Radicals (EPFRs). 1. Generation of Reactive Oxygen Species in Aqueous Solutions

Lavrent Khachatryan, Eric Vejerano, Slawo Lomnicki, and Barry Dellinger

Louisiana State University, Department of Chemistry and LSU Superfund Research Center, Baton Rouge, LA 70803

Abstract

Reactive oxygen species (ROS) generated by environmentally persistent free radicals (EPFRs) of 2-monochlorophenol, associated with CuO/silica particles, were detected using the chemical spin trap, 5,5-dimethyl-1-pyrroline-N-oxide (DMPO), in conjunction with Electron Paramagnetic Resonance (EPR) spectroscopy. Yields of hydroxyl radical ($\cdot\text{OH}$), superoxide anion radical ($\text{O}_2^{\cdot-}$), and hydrogen peroxide (H_2O_2) generated by EPFR-particle systems are reported. Failure to trap superoxide radicals in aqueous solvent, formed from the reaction of EPFRs with molecular oxygen, results from the fast transformation of the superoxide to hydrogen peroxide. However, formation of superoxide as an intermediate product in hydroxyl radical formation in aprotic solutions of dimethyl sulfoxide (DMSO) and acetonitrile (AcN) was observed. Experiments with superoxide dismutase (SOD) and catalase (CAT) confirmed the formation of superoxide and hydrogen peroxide, respectively, in the presence of EPFRs. The large number of hydroxyl radicals formed per EPFR and monotonic increase of the DMPO-OH spin adduct concentration with the incubation time suggest a catalytic cycle of ROS formation.

Keywords

Fly-ash; PM2.5; fine particles; combustion; thermal treatment; hazardous waste; hazardous materials; Superfund sites

Introduction

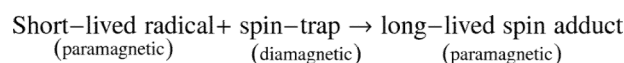
Environmentally persistent free radicals (EPFRs) have been shown to form on the surfaces of particles containing transition metal oxides and be capable of initiating adverse health impacts¹⁻³. The particles containing EPFRs generate DNA damage and induce pulmonary dysfunction consistent with free radical reactivity¹⁻⁵. These adverse effects are believed to result from the onset of oxidative stress initiated by EPFRs and are consistent with the oxidative stress-induced health impacts of exposure to airborne fine and ultrafine particulate matter (PM) and smoking^{1, 4, 5}. Oxidative stress is a result of above normal concentrations of reactive oxygen species (ROS) such as superoxide anion radical ($\text{O}_2^{\cdot-}$), hydrogen peroxide (H_2O_2), hydroxyl ($\cdot\text{OH}$), alkoxy ($\text{RO}\cdot$), peroxy ($\text{RO}_2\cdot$), and semiquinone, $\text{Q}^{\cdot-}$ radicals.

Since EPFRs induce oxidative stress in living cells they should promote ROS formation in aqueous media. However the detection of ROS species in aqueous media is challenging, as their half-lives, depending on the media, may be as short as 10^{-9} sec for $\cdot\text{OH}$, 10^{-6} sec for $\text{RO}\cdot$, and a few seconds for $\text{RO}_2\cdot$ and $\text{Q}^{\cdot-}$ ⁶. The half-life of $\text{O}_2^{\cdot-}$ depends strongly on media components (presence of superoxide dismutase - SOD, ROS etc⁶), and the dismutation of $\text{O}_2^{\cdot-}$ is essentially complete within 1 sec at pH=7.4⁷. This manuscript presents experimental evidence for the formation of ROS in the presence of EPFRs of 2-monochlorophenol

associated with copper oxide-containing silica particles in phosphate buffered saline (PBS) solutions using a 5,5-dimethyl-1-pyrroline-N-oxide (DMPO) spin-trapping agent in conjunction with EPR spectroscopy^{8, 9}.

Experimental Section

The spin-trapping process is based on a reaction between the spin trap molecule and a radical to produce a stable paramagnetic aminoxyl (or nitroxyl) species, which is referred to as a spin adduct. The spin trapping method for identifying radicals is based on a simple principle:



and takes advantage of the stability of the nitroxyl radicals. The aminoxyl product has a unique EPR spectrum which is dependent on the nature of the short-lived radical. In principle, any short-lived radical which is trapped can be unambiguously identified. In practice, however, there are some adducts which are difficult to assign.

Materials

High purity 5,5-dimethyl-1-pyrroline-N-oxide (DMPO, 99 %+, GLC) was obtained from ENZO Life Sciences International and used without further purification. Superoxide dismutase (SOD) from bovine erythrocytes, 3619 U/mg; catalase (CAT) from bovine liver, 3809 U/mg; desferrioxamine (DFO, assay 92.5%+, TLS); diethylenetriaminepentaacetic acid (DETAPAC, 99%+), dimethyl sulfoxide (DMSO, 99.7%+); 2-monochlorophenol (2-MCP, 99%+); copper nitrate hemipentahydrate (99.9%+); 0.01M phosphate buffered saline (PBS, NaCl 0.138M: KCl 0.0027M); 4-hydroxyl-2,2,6,6-tetramethylpiperidine-1-oxyl (TEMPOL, assay 97%+), and acetonitrile (AcN, 99.8%+) were all obtained from Sigma-Aldrich. Hydrogen peroxide was obtained from Fluka (Assay, 30%) and Cab-O-Sil™ from Cabot (EH-5, 99%).

EPFR-Particle System Preparation ¹⁰

Particles of 5 % CuO/silica (4 % Cu) were prepared by impregnation of silica powder (Cab-O-Sil) with 0.1 M solution of copper nitrate hemipentahydrate and calcinated at 450 °C for 12 h. The sample was then ground and sieved (mesh size 230, 63 μm). Prior to exposure, the particles were *heated in situ* in air to 450 °C for 1h to remove organics. The particles were exposed to saturated vapors of 2-MCP at 230 °C using a custom-made vacuum exposure chamber for 5 min. They were then cooled to 150 °C for 1 h at 10⁻² torr. This process resulted in the formation of EPFR-metal complexes (cf. Figure 1) which depicts how three different EPFRs can be formed on the CuO/silica surface, viz. 2-chlorophenoxy-Cu(I), 2-hydroxyphenoxy-Cu(I), and *o*-semiquinone radical-Cu(I) by reaction of the hydroxyl substituent, the chlorine substituent, or both substituents, respectively ¹⁰. EPR spectra were then acquired at ambient condition to confirm the existence of EPFRs. The average radical concentration (spins/g of CuO/Silica) was computed from averaging three EPR measurements of 2-monochlorophenol dosed onto Cu(II)O/silica, weighing 100 mg for each trial. The concentration was calculated using DPPH as a standard due to the similarity of the spectral profiles of DPPH and the radicals formed on silica. The double integrated intensity of the first-derivative EPR spectra was used and interpolated from a four-point DPPH calibration standard (plotted as double-integrated intensity vs amount of DPPH (ug)) to determine the amount of the radical, and converted to the number of spins by multiplying by the Avogadro's number and suitable conversion factor. The final concentration was

determined by dividing the # of spins with the total amount of sample (CuO/silica) which is 0.100 g. The average quantified amounts of adsorbed radicals on Cu(II)O/silica reached $\sim 10^{17}$ (spins/g).

Undosed Cu(II)O/silica particles, which did not contain EPFRs, were used as control solution (non-containing EPFRs).

***In-Vitro* Studies**

1 mg/ml suspensions of the control (non-containing EPFRs, i.e CuO/silica), and sample, EPFR/CuO/silica, were prepared in water, DMSO, or AcN and saturated with air by bubbling air for 5 minutes. Prior to adding DMPO, the surrogate solutions were sonicated 5 minutes (Fisher Scientific, FS-20) at 40 W. A phosphate buffered saline (PBS, 0.01M) was used to maintain the pH at 7.4 and balance the final volume at 200 μ l. The order of introduction of final solution components to PBS was: particle suspension (10 μ l from solution of 1 mg/ml) + DMPO (10 μ l from solution of 3 M) + reagents + buffer to balance at 200 μ l. The final composition of the suspension in most experiments was (50 μ g/ml) particles + DMPO (150 mM) + reagent (200 μ l).

Different biological reagents were used in specific experiments: SOD, CAT, and metal chelators. Solutions were kept in the dark and shaken in touch mode for 30 s using a Vortex Genie 2 (Scientific Industries). A 20 μ l aliquot was transferred to an EPR capillary tube (i.d. \sim 1mm, o.d. 1.55mm) and sealed at one end with sealant (Fisherbrand). The capillary was inserted in a 4 mm EPR tube and inserted into the EPR resonator¹¹. The intensities of the spectra were reported in arbitrary units, DI/N, i.e., a double integrated (DI) intensity of the EPR spectrum normalized (N) to account for the conversion time, receiver gain, number of data points and sweep width [<http://www.bruker-biospin.com/winepr.html?&L=0>]). Each experiment was performed at least twice, and the final EPR spectrum represents an average of all spectra obtained for each experiment.

Since the chemistry of interaction of chelators with the surface of the model particles is unclear, we abstained from the use of chelators such as Desferrioxamine (DFO), DETAPAC, EDTA, which minimize the iron content in solution. Chelators can change the reactivity of particles drastically by affecting their redox potential of metals¹². Chelators may also affect the extraction of adsorbed EPFRs by forming metal-chelate complexes. The oxidizing species formed by the Fenton-type reaction are known to be affected by iron chelators^{13,14}. For instance, in the case of DFO, some additional secondary actions have been demonstrated, particularly scavenging of semiquinone-type radicals and stimulation of the hydrolysis of some halogenated substituents¹⁵. The potential removal of iron from the *in-vitro* test solutions may inhibit Fenton-type reactions that contribute to ROS yield. However, the buffer, prepared in deionized water and treated with Chelex 100 ion-exchange resin (Bio-Rad Laboratories, Hercules, LA) to remove trace heavy metal contaminants¹⁶, did not have a significant impact on the spin trapping results.

EPR Measurements

EPR spectra were recorded using a Bruker EMX-20/2.7 EPR spectrometer (X-band) with dual cavities and modulation and microwave frequencies of 100 kHz and 9.516 GHz, respectively. Typical parameters were: sweep width--100 G, EPR microwave power-- 10 mW, modulation amplitude--0.8 G, time constant--40.96 ms, and sweep time-- 167.77s.

Values of the g-tensor were estimated using Bruker's WIN-EPR SimFonia 2.3 program, which is a comprehensive line of software, allowing control of the Bruker EPR spectrometer, data-acquisition, automation routines, tuning, and calibration programs on a Windows-based PC [<http://us.bruker-biospin.com/brukerepr/winepr.html>]. The exact g-

values for key spectra were determined by comparison with 2,2-diphenyl-1-picrylhydrazyl (DPPH) standard.

Calculation of OH Radical Concentration

EPR spectra of DMPO-OH adducts were recorded. It was assumed that one mole DMPO-OH adduct corresponds to one mole •OH in solution. The DMPO-OH radical adduct concentration was determined by double integration of the second line (at low magnetic field) of their respective 4 line spectra and compared to the intensity of the 4-hydroxyl-2,2,6,6-tetramethylpiperidine-1-oxyl, TEMPOL (stable radical) standard. The standard Tempol (0.05 – 1 mM) solution was used, with calibration based on double integration of the second line of Tempol's 3 line EPR spectra at low magnetic field¹⁷. The Tempol concentration was verified by Agilent 8453 UV-Visible Spectrophotometer using the extinction coefficient of $13.2 \pm 0.1 \text{ M}^{-1}\text{-cm}^{-1}$ at 436 nm¹⁷.

Processing of EPR Spectra from the Literature

UN-SCAN-IT Automated Digitizing System, Version 6.0 (Silk Scientific Corporation, <http://www.silkscientific.com/>) was used to digitize scanned EPR spectra published in the literature. The absolute value of the resonance field is different for each original spectrum due to use of different microwave frequencies. To facilitate comparison of spectra, all experimental and literature X-band spectra were recreated on the same field scale, generally in a 100-G wide field window.

Results and Discussion

Hydroxyl radical generation

Electron transfer from the EPFR to molecular oxygen was hypothesized to form superoxide radical ion, then hydrogen peroxide and hydroxyl radical via dismutation and Fenton Reactions, respectively, via the simple pathway in Scheme 1. The identification of the •OH in the aqueous solutions containing EPFRs and their relative concentration compared to the control (non-containing EPFRs) was measured using the DMPO spin trap.

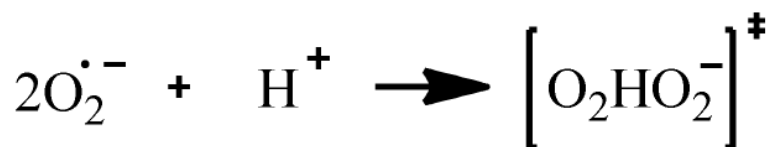
The 4-line EPR spectrum characteristic of DMPO-OH adducts was detected in solutions containing both EPFR or non-EPFR particles with DMPO in PBS media (cf. Figure 2A), the EPFR-containing particles initially producing only slightly more DMPO-OH adducts than the control particles. However, the difference DMPO-OH spin adduct formed in the presence of EPFR-containing particles and the controls increased with increasing incubation time (cf. Figure 2B). On average, twice as much DMPO-OH spin adduct was formed in the presence of EPFR-containing particles than the control (non-containing EPFRs) particles at longer incubation times. The greatest difference in hydroxyl radical concentration occurred at incubation times of greater than 12 hours.

The concentration of hydroxyl radicals generated by the EPFR-particle system might be considered to be the difference between DMPO-OH adducts formed in EPFR-containing particles and the non-EPFR particles. However, there are no literature reports of the generation of hydroxyl radicals in fresh solution of CuO/SiO₂ (control particles). Even with the addition of hydrogen peroxide, the formation of hydroxyl radical could not be confirmed in an Cu(II)O_(aq)/H₂O₂ reaction system, despite the detection of a prominent signal DMPO-OH adduct due to the nucleophilic addition of water to DMPO¹⁸. The non-radical nucleophilic reaction of water with DMPO is known to be a significant pathway to the formation of DMPO-OH radical adduct^{19,20}. The direct hydroxylation of DMPO in water media via nucleophilic attack of water by non-hydroxyl oxidants such as H₂O₂, Fe and Cu ions, and other catalysts may readily occur^{21,22}. Thus, baseline DMPO-OH concentration in

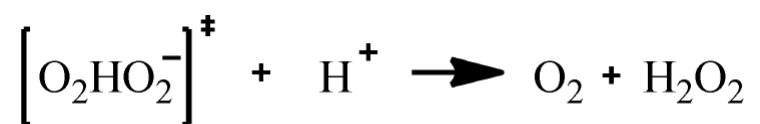
the CuO/silica control (non-containing EPFRs) samples is probably due to nucleophilic addition of water to CuO, and the difference in concentration of DMPO-OH adducts between solutions of EPFR-containing particles and control particles can be attributed to formation of hydroxyl radicals in EPFR-particle systems containing solutions.

The concentration of hydroxyl radicals was quantified with the assumption of 1-to-1 hydroxyl radical-to-DMPO stoichiometry for DMPO-OH spin adduct formation and calibration using a Tempol solution as a standard. The hydroxyl radical concentration was calculated to be 1.39×10^{14} spins/ml (0.23 μM) at an incubation time of 140 minutes. This may be considered a lower concentration limit because of the decay of DMPO-OH during accumulation as well as the effectiveness of trapping hydroxyl radicals by DMPO. Similar micromolar concentrations (up to 1 μM) of hydroxyl radical have been detected in solution from airborne particulate matter (urban dust SRM 1649, Washington DC area) and diesel particulate matter (SRM 2975) using a high sensitivity fluorescence method²³. Up to 2 μM of DMPO-OH adducts have been reported from Fenton reaction mixtures (10 μM Fe(II)SO₄+100 μM DMPO+80 μM H₂O₂)¹³ and up to 1 μM DMPO-OH adduct for Fenton reaction mixtures containing 1 μM Fe⁺²²⁴.

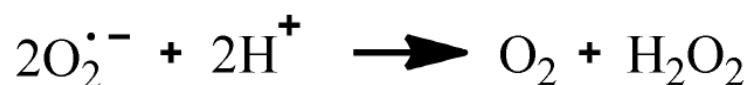
Comparison of the concentration of hydroxyl radicals to EPFR radicals: $[\text{OH}] / [\text{EPFRs}'] = 1.39 \times 10^{14}$ (spins/ml) / 150×10^{-6} (g/ml) $\times 10^{17}$ (spins/g) indicates that 1 EPFR generates ~ 10 hydroxyl radicals at an incubation time of 140 min. The monotonic increase in the number of DMPO-OH adducts with the incubation time as well as the large number of hydroxyl radicals formed per EPFR suggests a catalytic cycle of hydroxyl radical formation.



rxn 1



rxn 2



rxn 3

The effect of SOD and CAT

The principal source of hydroxyl radicals in the presence of EPFRs outside of the biological systems is probably superoxide dismutation, reactions 1-3, resulting in the formation of hydrogen peroxide^{25, 26}. The overall reaction is usually a second order process, where one superoxide molecule transfers an electron to another superoxide molecule with the

generation of excessive charge density being avoided by the involvement of a proton²⁵. This reaction has been proven to occur over a very broad pH range (5-10). The reaction involves the incorporation of a single proton into the transition state $[\text{O}_2\text{HO}_2^-]^\ddagger$, rxn 1. The overall rate of superoxide dismutation, a second order reaction²⁷, is usually slow in aqueous media ($k_3 \sim 10^5 \text{ M}^{-1}.\text{s}^{-1}$ at pH = 7.4^{25, 26}) and is catalyzed by the presence of transition metals. For example, k_3 may increase from 10^6 to $10^9 \text{ M}^{-1}.\text{s}^{-1}$ in presence of copper containing compounds^{26, 27}. We have unsuccessfully attempted to spin-trap superoxide radicals in aqueous solutions containing either EPFR or non-EPFR particles using a DMPO spin trapping agent. This is probably due to a fast dismutation of superoxide catalyzed by CuO/silica as well as a very short lifetime (less than 1 min at pH = 7.4²⁸) of the DMPO – superoxide adduct (abbreviated as DMPO-OOH at neutral and higher pH media in aqueous solution and as DMPO- O_2^- in aprotic solutions²⁹).

One of the biological agents for the decomposition of superoxide is the enzyme superoxide dismutase (SOD), a soluble, copper-protein complex, with a superoxide decomposition rate constant of $1.3 \times 10^9 \text{ M}^{-1}.\text{s}^{-1}$ ²⁷. Therefore the SOD may accelerate the rate of rxn 3 by about 4 orders of magnitude in aqueous media and can be used as an effective indicator of superoxide involvement in the current experiments by inhibiting the sequence: $\text{O}_2^{\cdot-} \rightarrow \text{H}_2\text{O}_2 \rightarrow \cdot\text{OH} \rightarrow \text{DMPO-OH}$. Although SOD transforms superoxide into H_2O_2 , the interaction between peroxide and SOD has been studied as a function of overall activity loss³⁰. As a result less DMPO-OH adducts may appear during the process. Otherwise, other mechanisms may be responsible for DMPO-OH formation³¹.

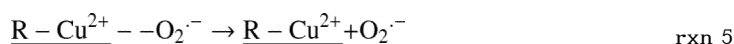
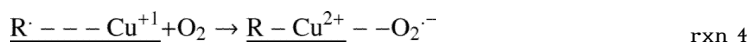
Standard procedure to verify the existence of superoxide radicals and hydrogen peroxide molecules is to introduce SOD and CAT working solutions and observe a decrease in superoxide concentration. CAT converts hydrogen peroxide into water and oxygen, and thus its addition to the reaction system will also diminish hydroxyl radical formation, though at a different stage of the process. In the current experiment, both SOD and CAT should decrease the DMPO-OH adduct concentration if DMPO-OH forms in the sequence $\text{O}_2^{\cdot-} \rightarrow \text{H}_2\text{O}_2 \rightarrow \cdot\text{OH} \rightarrow \text{DMPO-OH}$ ^{30, 31}.

The results of introduction of CAT, SOD (20 $\mu\text{g/ml}$ (70 U/ml) to 80 $\mu\text{g/ml}$ (280 U/ml)³²⁻³⁴) and both CAT and SOD together to the solutions containing EPFR-particle systems are presented in Figure 3. Both SOD and CAT individually decreased the DMPO-OH adduct concentration in solution. Introduction of SOD and CAT together resulted in a significantly greater reduction of the DMPO-OH adduct concentration. These results unambiguously demonstrate the interconnection of superoxide and hydrogen peroxide formed from EPFRs.

Trapping of $\text{O}_2^{\cdot-}$ by DMPO in aprotic solvents

The effect of SOD on the formation of DMPO-OH adduct in the presence of EPFR particles strongly suggested the involvement of superoxide radicals, even though the radicals could not be spin-trapped in the aquatic media. Unfortunately, the commonly used nitron spin traps (DMPO as well) have a very low efficacy for trapping superoxide radicals in aqueous media and the DMPO-superoxide radical adduct (DMPO-OOH) is not stable^{35, 36, 29, 36, 37}. However, since superoxide has considerable nucleophilic character in aprotic solvents^{25, 38}, the application of such solvents may facilitate their trapping. One concern in this approach is that while o-semiquinone radicals are known to be generated in aqueous media where the radical-anion is readily formed³², it is unclear if it occurs in aprotic solvents where the radical anion may not be stabilized and the effect of the metal on EPFRs is unknown (*vide infra*, Figure 5). The o-semiquinone radical bound to the Cu(I) center (Figure 1) can be considered a radical anion because of the high polarity of the nonradical-bearing oxygen-copper bond. Accordingly, the reaction of O_2 with the o-semiquinone type EPFRs should yield superoxide, even in aprotic media.

However, superoxide may also be generated by initial complexation and subsequent reaction of O₂ with the lower valence state transition metal complex formed at the site of chemisorption of the EPFR precursor to the transition metal. (cf. Rxns. 4 and 5) where R· represents the semiquinone radical and R represents the non-radical, chemisorbed organic in Figure 1.^{25, 38}



Due to their affinities for superoxide, we have performed experiments in aprotic dimethylsulfide (DMSO)^{38, 39} and AcN solvents⁴⁰. Solubility of oxygen in these solvents, follows the order: H₂O < DMSO < AcN⁴⁰⁻⁴²; and the calculated rate constant of interaction of superoxide with DMPO in different media is also in the order: H₂O (5.85 × 10⁻⁵ M⁻¹ s⁻¹) < DMSO (8.71 × 10⁻⁴ M⁻¹ s⁻¹) < AcN (1.81 × 10⁻³ M⁻¹ s⁻¹)²⁹. Both results suggest spin trapping of superoxide with DMPO will be more effective in AcN and DMSO than water.

The results of the DMPO-O₂^{·-} spin adduct formation in these solvents are summarized in Figure 4. A weak signal was detected in the solution of EPFR-particle systems in DMSO (Figure 4A, spectrum 2), while a broad, 4-line signal was detected in AcN solution (Figure 4A, spectrum 3). This is typical for DMPO-O₂^{·-} adduct in suspensions of powdery semiconductors (TiO₂, Fe₂O₃, WO₃, CdS) in AcN⁴⁰. Such broadening of the DMPO-O₂^{·-} spectra might be explained by high concentration of oxygen in AcN and interaction of oxygen with the paramagnetic DMPO-O₂^{·-} probe signal³⁵. The resolution of this spectrum was improved when the same experiment was repeated with a smaller amount of the EPFR suspended in solution (Figure 4A, spectrum 4). The EPR spectrum of DMPO-O₂^{·-} spin adduct formed by photoexcitation of powdery semiconductor TiO₂ in AcN solution⁴⁰ (Figure 4B, red line) fits well with our experimental DMPO-O₂^{·-} spectrum (Figure 4B, black line) for the EPFR-particle system. These results provide direct proof of formation of superoxide from molecular oxygen in the presence of EPFR-particle systems.

The polarity effects of solvents on hyperfine splitting constants (hfsc) of DMPO-O₂^{·-} adducts (spectra 2 and 4) are visible when compared to the EPR spectra of DMPO-O₂^{·-} spin adduct from the Fenton reaction in 70% DMSO in water (spectrum 1). The hfsc values are: α_N = 14.50 G, α_H^β = 10.67 G, α_H^β = 1.40 G²², α_N = 14.00 G, α_H^β = 9.8 G, α_H^β = 1.40 G (this work) for DMPO-superoxide radical in DMSO, and α_N = 13.00 G and α_H^β = 9.0 G (this work) for DMPO-superoxide radical in AcN for spectra 1, 2, and 4, respectively. We were unable to determine the value of α_H^β in AcN. This is probably due to the high concentration of dissolved oxygen which contributes to the broadening of the spectra in AcN⁴⁰. The decrease of the hfsc values for DMPO-O₂^{·-} in different solvents, correlates with decreasing solvent polarity of the solvent. According to Burdick and Jackson's polarity index⁴³, the solvent's polar property is as follows: H₂O [10.2] > DMSO [7.2] > acetonitrile [5.8], with the polarity indexes given in parentheses. In agreement with the polarity, the highest hfsc values were detected in water and the lowest in acetonitrile. The inability to detect superoxide radicals in the aquatic media, while a DMPO-O₂^{·-} spin adduct was readily detected in aprotic solvents, suggests a very rapid reactions of superoxide in an aqueous environment.

Additional experiments with AcN-water solutions in various proportions indicate even small amounts of water result in immediate formation of hydroxyl radical and detection of DMPO-OH spin adduct product (cf. Table 1). Concomitantly, the characteristic ΔH_p -p for DMPO-OH adduct (for the second intense line at low magnetic field) is increased with the addition of AcN from ~ 1.2 G in pure aqueous solution, to 1.3 G in 20 % AcN, and 1.8 G in 50 % AcN. The hfsc values decrease from 14.95 G in pure water to 14.28 B in 50% AcN. The changes within the EPR spectra upon introduction of aprotic solvent to the water solution are related to the high concentration of oxygen in AcN as well as its high polarity and possibly some superposition of spectra DMPO-OH and DMPO-OOH²². These results indirectly show that the superoxide anions are self-dismutated in protic environment²⁵ and form hydroxyl radicals by Scheme 1.

The body of work of Pryor *et al.* indicates semiquinone radicals can mediate, and perhaps catalyze, the formation of ROS in biological systems⁴⁴⁻⁴⁶. The EPFR-transition metal systems, which we have shown to form, have the added component of a redox-active transition metal⁴⁷⁻⁴⁹, and EPFR-copper oxide systems have been demonstrated to induce oxidative stress resulting in pulmonary and cardiac dysfunction in mice and rats⁵⁰⁻⁵². This leads us to hypothesize that the combination of EPFR and redox-active transition metals can catalyze the formation of various types of ROS. The Fenton reaction, in which a reduced metal mediates the conversion of hydrogen peroxide to hydroxyl radical, is likely a key component¹⁴. Fenton reactions involving endogenous Fe (II) are frequently invoked to form ROS in biological systems^{24, 26}. However, our EPFR-transition metal systems have the reduced metal located in the immediate vicinity of the EPFR which may promote their synergistic, purely exogenous, effects. ROS generation has been shown to increase in the presence of environmental particulate matter and the involvement of environmental Fe(II) has been invoked^{46, 47}. However, the iron in However, as depicted in Figure I, Cu(II) is reduced to Cu(I) as EPFRs are formed. Cu(I) is Fenton-active^{18, 53} and can participate in ROS-generating cycles similarly to Fe (II).

Based on our research and contributions from the literature, reaction cycles in which EPFR-transition metal complexes generate superoxide radical anion, hydroxyl radical, and other ROS can be envisioned (cf. Figure 5 for the example of 2-monochlorophenol-CuO system). **Cycle I** depicts how 2-hydrophenoxy radical (**D**) can catalytically generate ROS under biological conditions with regeneration of 2-hydrophenoxy radical. **Cycle II** depicts how o-semiquinone radical (**E**) can also generate superoxide and hydroxyl radical. However in this cycle, o-semiquinone radical (**E**) is not regenerated under biological conditions because conversion of species **F** back to o-semiquinone radical (**E**) requires temperatures above 150 C⁴⁹. However, formation of species **F** can contribute to **Cycle 1**. It is remarkable that both the complete **Cycle 1** and the auxiliary **Cycle II** may operate in aqueous media to generate ROS. It is also worthy to note that because o-semiquinone radical (**E**) can also be considered to be a radical anion, the reaction of O₂ with **E** will yield superoxide (red arrow), even in aprotic media.

Acknowledgments

The authors gratefully acknowledge the partial support of this research under NIEHS Grant (Superfund Research and Training Program) PES013648Z.

Abbreviations

AcN	acetonitrile
CAT	(bovine) catalase

DETAPAC	diethylenetriaminepentacetic acid
DFO	desferrioxamine
DMSO	dimethyl sulfoxide
DMPO	5,5-dimethyl-1-pyrroline-1-oxide
EPFR	environmentally persistent free radical
EPR	electron paramagnetic resonance
SOD	(bovine) superoxide dismutase

References

- (1). Dellinger B, Pryor WA, Ceuto R, Squadrito GL, Hedge V, Deutsch WA. Role of free radicals in the toxicity of airborne fine particulate matter. *Chem Res Toxicol.* 2001; 14:1371–1377. [PubMed: 1159928]
- (2). Maskos Z, Khachatryan L, Dellinger B. Precursors of radicals in tobacco smoke and the role of particulate matter in forming and stabilizing radicals. *Energy Fuels.* 2005; 19:2466–2473.
- (3). Knaapen AM, Shi TM, Borm PJA, Schins RPF. Soluble metals as well as the insoluble particle fraction are involved in cellular DNA damage induced by particulate matter. *MolCellBiochem.* 2002; 234(1):317–326.
- (4). Dellinger B, Pryor WA, Cueto R, Squadrito GL, Deutsch WA. Combustion-generated radicals and their role in the toxicity of fine particulate. *Organohal Comp.* 2000; 46:302–305.
- (5). Cormier SA, Lomnicki S, Backes W, Dellinger B. Origin and health impacts of emissions of toxic by-products and fine particles from combustion and thermal treatment of hazardous wastes and materials. *EnvironHealth Perspect.* 2006; 114:810–817.
- (6). Pryor WA. Oxy-Radicals and Related Species: Their Formation, Lifetimes, and Reactions. *Annual Review of Physiology.* 1986; 48:657–667.
- (7). Finkelstein E, Rosen GM, Rauckman EJ. Production of Hydroxyl Radical by Decomposition of Superoxide Spin-Trapped Adducts. *Molecular Pharmacology.* 1982; 21(2):262–265. [PubMed: 6285165]
- (8). Forshult S, Lagercræ C. Use of Nitroso Compounds as Scavengers for Study of Short-Lived Free Radicals in Organic Reactions. *Acta Chemica Scandinavica.* 1969; 23(2):522. &
- (9). Janzen EG, Blackburn BJ. Detection and Identification of Short-Lived Free Radicals by an Electron Spin Resonance Trapping Technique. *J.Am.Chem.Soc J1 - JACS.* 1968; 90(21):5909. &
- (10). Truong H, Lomnicki S, Dellinger B. Potential for Misidentification of Environmentally Persistent Free Radicals as Molecular Pollutants in Particulate Matter. *Environmental Science & Technology.* 2010; 44(6):1933–1939. [PubMed: 20155937]
- (11). Nakagawa K. Is quartz flat cell useful for the detection of superoxide radicals? *J Act Oxyg Free Rad.* 1994; 5:81–85.
- (12). Fubini B, Mollo L, Giamello E. Free radical generation at the solid/liquid interface in iron containing minerals. *Free Rad Res.* 1995; 23(6):593–614.
- (13). Tomita M, Okuyama T, Watanabe S, Watanabe H. Quantitation of the Hydroxyl Radical Adducts of Salicylic-Acid by Micellar Electrokinetic Capillary Chromatography - Oxidizing Species Formed by a Fenton Reaction. *Archives of Toxicology.* 1994; 68(7):428–433. [PubMed: 7979959]
- (14). Yamazaki I, Piette LH. EPR Spin-Trapping Study on the Oxidizing Species Formed in the Reaction of the Ferrous Ion with Hydrogen-Peroxide. *J.Am.Chem.Soc J1 - JACS.* 1991; 113(20): 7588–7593.
- (15). Zhu BZ, Har-El R, Kitrossky N, Chevion M. New modes of action of desferrioxamine: scavenging of semiquinone radical and stimulation of hydrolysis of tetrachlorohydroquinone (vol 24, pg 360, 1997). *Free Radical Biology and Medicine.* 1998; 24(5):880.

- (16). Finkelstein E, Rosen GM, Rauckman EJ. Spin Trapping - Kinetics of the Reaction of Superoxide and Hydroxyl Radicals with Nitrones. *J. Am. Chem. Soc.* 1980; 102(15):4994–4999.
- (17). Yordanov ND, Rangelova K. Quantitative electron paramagnetic resonance and spectrophotometric determination of the free radical 4-hydroxy-2,2,6,6-tetramethylpiperidinyloxy. *Spectrochimica Acta Part a-Molecular and Biomolecular Spectroscopy.* 2000; 56(2):373–378.
- (18). Burkitt MJ, Tsang SY, Tam SC, Bremner I. Generation of 5,5-Dimethyl-1-Pyrroline N-Oxide Hydroxyl and Scavenger Radical Adducts from Copper/H₂O₂ Mixtures - Effects of Metal-Ion Chelation and the Search for High-Valent Metal-Oxygen Intermediates. *Arch. Biochem. Biophys.* 1995; 323(1):63–70. [PubMed: 7487075]
- (19). Hanna PM, Chamulitrat W, Mason RP. When Are Metal Ion-Dependent Hydroxyl and Alkoxy Radical Adducts of 5,5-Dimethyl-1-Pyrroline N-Oxide Artifacts. *Arch. Biochem. Biophys.* 1992; 296(2):640–644. [PubMed: 1321591]
- (20). Chamulitrat W, Iwahashi H, Kelman DJ, Mason RP. Evidence against the 1-2-2-1 Quartet Dmpo Spectrum as the Radical Adduct of the Lipid Alkoxy Radical. *Arch. Biochem. Biophys.* 1992; 296(2):645–649. [PubMed: 1321592]
- (21). Finkelstein E, Rosen GM, Rauckman EJ. Spin Trapping of Superoxide and Hydroxyl Radical - Practical Aspects. *Arch. Biochem. Biophys.* 1980; 200(1):1–16. [PubMed: 6244786]
- (22). Makino K, Hagiwara T, Murakami A. Fundamental-Aspects of Spin Trapping with Dmpo. *Radiation Physics and Chemistry.* 1991; 37(5-6):657–665.
- (23). Alaghmand M, Blough NV. Source-dependent variation in hydroxyl radical production by airborne particulate matter. *Environmental Science & Technology.* 2007; 41(7):2364–2370. [PubMed: 17438788]
- (24). Yamazaki I, Piette LH. ESR Spin-Trapping Studies on the Reaction of Fe²⁺ Ions with H₂O₂ Reactive Species in Oxygen-Toxicity in Biology. *Journal of Biological Chemistry.* 1990; 265(23):13589–13594. [PubMed: 2166035]
- (25). Fee, JA.; Valentine, JS. Chemical and Physical Properties of Superoxide. In: Michelson, AM.; McCord, JM.; Fridovich, I., editors. *Superoxide and Superoxide Dismutases.* Academic Press; New York: 1977. p. 19-60.
- (26). Halliwell B, Gutteridge JMC. Free Radicals and Metal Ions in Human Disease in *Methods in Enzymology.* 1990; 186:1–85. [PubMed: 2172697]
- (27). Bielski BHJ, Allen AO. Mechanism of Disproportionation of Superoxide Radicals. *J. Phys. Chem.* 1977; 81(11):1048–1050.
- (28). Buettner GR, Oberley LW. Considerations in Spin Trapping of Superoxide and Hydroxyl Radical in Aqueous Systems Using 5,5-Dimethyl-1-Pyrroline-1-Oxide. *Biochemical and Biophysical Research Communications.* 1978; 83(1):69–74. [PubMed: 212052]
- (29). Villamena FA, Xia S, Merle JK, et al. Reactivity of superoxide radical anion with cyclic nitrones: Role of intramolecular H-bond and electrostatic effects. *J. Am. Chem. Soc.* 2007; 129(6):8177–8191.
- (30). Cabelli DE, Allen D, Bielski BHJ, Holcman J. The Interaction between Cu(I) Superoxide-Dismutase and Hydrogen-Peroxide. *Journal of Biological Chemistry.* 1989; 264(17):9967–9971. [PubMed: 2722888]
- (31). Buettner GR, Mason RP, Cutler RG, Rodrigues H. Chapter 2. Critical reviews of oxidative stress and aging: Advances in basic science, diagnostics and intervention. 2003:27–38.
- (32). Zang LY, Stone K, Pryor WA. Detection of Free Radicals in Aqueous Extracts of Cigarette Tar by ESR. *Free Radical Biol Med.* 1995; 19:161–167. [PubMed: 7649487]
- (33). Pryor WA, Stone K, Zang L-Y, Bermudez E. Fractionation of Aqueous Cigarette Tar Extracts: Fractions that Contain the Tar Radical Cause DNA Damage. *Chem. Res. Toxicol.* 1998; 11:441–448. [PubMed: 9585474]
- (34). Arroyo CM, Kramer JH, Dickens BF, Weglicki WB. Identification of Free-Radicals in Myocardial-Ischemia Reperfusion by Spin Trapping with Nitron Dmpo. *Febs Letters.* 1987; 221(1):101–104. [PubMed: 3040465]

- (35). Roubaud V, Sankarapandi S, Kuppusamy P, Tordo P, Zweier JL. Quantitative measurement of superoxide generation using the spin trap 5-(diethoxyphosphoryl)-5-methyl-1-pyrroline-N-oxide. *Analytical Biochemistry*. 1997; 247(2):404–411. [PubMed: 9177705]
- (36). Dikalov SI, Dikalova AE, Mason RP. Noninvasive diagnostic tool for inflammation-induced oxidative stress using electron spin resonance spectroscopy and an extracellular cyclic hydroxylamine. *Arch.Biochem.Biophys*. 2002; 402(2):218–226. [PubMed: 12051666]
- (37). Bacic G, Spasojevic I, Secerov B, Mojovic M. Spin-trapping of oxygen free radicals in chemical and biological systems: New traps, radicals and possibilities. *Spectrochimica Acta Part a-Molecular and Biomolecular Spectroscopy*. 2008; 69(5):1354–1366.
- (38). Valentine, JS.; Foote, CS.; Grenbery, A.; Liebman, JFE. *Active oxygen in biochemistry*. Vol. 3. Blackie Academic & Professional; 1995.
- (39). Dvoranova D, Brezova V, Mazur M, Malati MA. Investigations of metal-doped titanium dioxide photocatalysts. *Appl Catal B*. 2002; 37(2):91–105.
- (40). Noda H, Oikawa K, Ohya-Nishiguchi H, Kamada H. Detection of superoxide ions from Photoexcited Semiconductors in Non-Aqueous solvents using ESR Spin-Trapping technique. *Bulletin of the Chemical Society of Japan*. 1993; 66(12):3542–3547.
- (41). Baird WR, Foley RT. Solubility of Oxygen in Selected Organic-Solvents. *Journal of Chemical and Engineering Data*. 1972; 17(3):355. &
- (42). Greenwald, R. A. *Handbook of Method for oxygen radical research*. CRC Press; Florida: 1985. p. 65
- (43). Lee, ML.; Markides, KE. *Chromatography Conferences. Inc.; Provo, Utah: 1990. Analytical Supercritical Fluid Chromatography and Extraction*.
- (44). Zang L-Y, Stone K, Pryor WA. Detection of free radicals in aqueous extracts of cigarette tar by electron spin resonance. *Free Radicals in Biology and Medicine*. 1995; 19(2):161–167.
- (45). Pryor WA, Stone K, Zang L-Y, Bermudez E. Fractionation of aqueous cigarette tar extracts: Fractions that contain the tar radicals cause DNA damage. *Chem Res Toxicol*. 1998; 11(5):441–448. [PubMed: 9585474]
- (46). Squadrito GL, Cueto R, Dellinger B, Pryor WA. Quinoid redox cycling as a mechanism for sustained free radical generation by inhaled airborne particulate matter. *Free Radical Biology and Medicine*. 2001; 31(9):1132–1138. [PubMed: 11677046]
- (47). Dellinger B, Pryor WA, Cueto R, Squadrito GL, Hedge V, Deutsch WA. Role of free radicals in the toxicity of airborne fine particulate matter. *Chem Res Toxicol*. 2001; 14:1371–1377. [PubMed: 11599928]
- (48). Dellinger B, Lomnicki S, Khachatryan L, et al. Formation and stabilization of persistent free radicals. *Proceedings of the Combustion Institute*. 2007; 31:521–528.
- (49). Lomnicki S, Truong H, Vejerano E, Dellinger B. Copper oxide-based model of persistent free radical formation on combustion-derived particulate matter. *Environmental Science & Technology*. 2008; 42(13):4982–498. [PubMed: 18678037]
- (50). Fahmy B, Ding L, You D, Lomnicki S, Dellinger B, Cormier SA. In vitro and in vivo assessment of pulmonary risk associated with exposure to combustion generated fine particles. *Environmental Toxicology and Pharmacology*. 2010; 29:173–182. [PubMed: 20369027]
- (51). Balakrishna S, Lomnicki S, McAvey KM, Cole RB, Dellinger B, Cormier SA. Environmentally persistent free radicals amplify ultrafine particle mediated cellular oxidative stress and cytotoxicity. *Particle Fibre and Toxicology*. 2009; 6:11.
- (52). Balakrishna S, Lomnicki S, Dellinger B, Cormier SA. Resveratrol Ameliorates the Redox Imbalances in Human Airway Epithelial Cells Exposed to Combustion Generated Nanoparticles. *Free Radical Biology and Medicine*. 2008; 45:S44–S.
- (53). Masarwa M, Cohen H, Meyerstein D, Hickman DL, Bakac A, Espenson JH. Reactions of Low-Valent Transition-Metal Complexes with Hydrogen-Peroxide - Are They Fenton-Like or Not .1. The Case of Cu+Aq and Cr-2+Aq. *J.Am.Chem.Soc J1 - JACS*. 1988; 110(13):4293–4297.

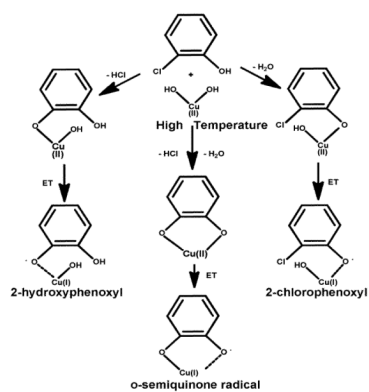


Figure 1. EPFR-metal systems formed on SiO₂ from the chemisorption of 2-MCP. ET-Electron transfer.

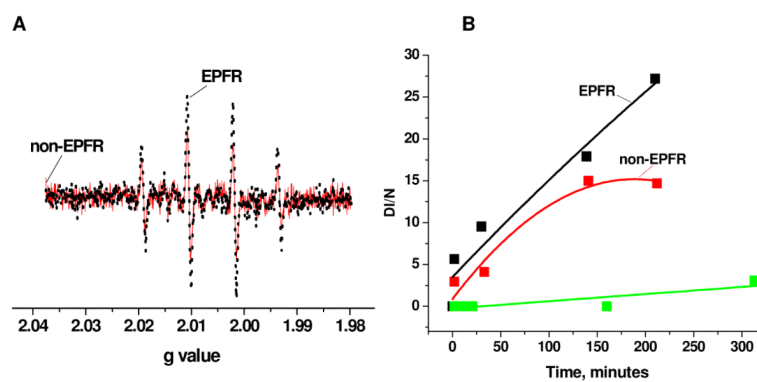


Figure 2.

A. Comparison of the EPR signal intensity of DMPO-OH adduct in the presence of EPFR-containing particles (black) and control (non-containing EPFRs) particles (red). B. Evolution of the DMPO-OH adducts signal intensity in the presence EPFR-containing particles (black), control particles (red) and in the absence of particles (green).

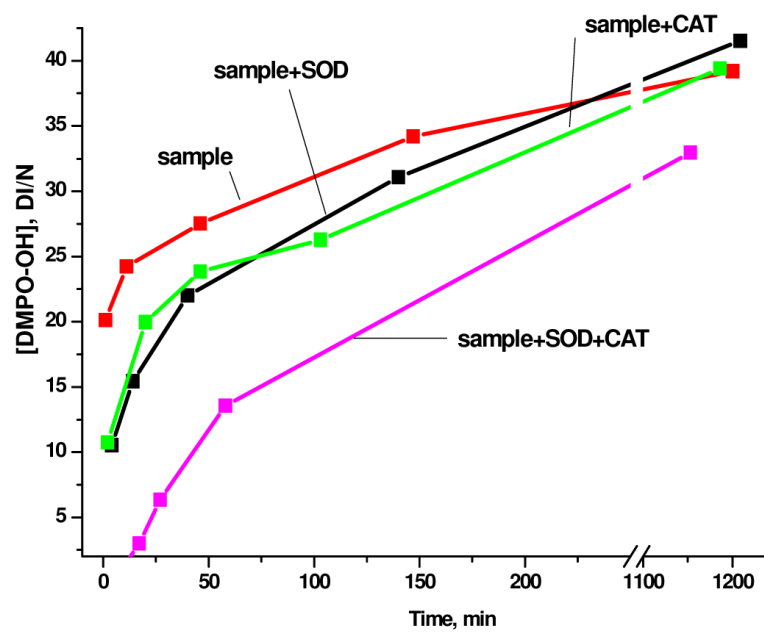


Figure 3. The inhibition effect of 80 $\mu\text{g/ml}$ SOD (280 U/ml) and 80 $\mu\text{g/ml}$ CAT (280 U/ml) on the Sample solution (EPFRs (50 $\mu\text{g/ml}$) + DMPO 150 mM + buffer).

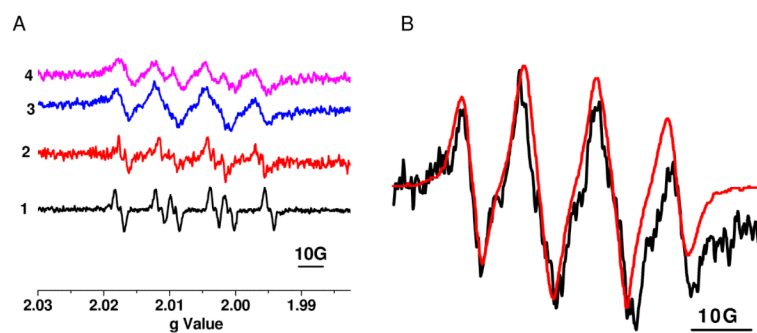


Figure 4.

A) *Spectrum 1* DMPO-O₂⁻ from Fenton reaction *. *Spectrum 2* - DMPO-O₂⁻ adduct formed in DMSO media with 50 ug/ml EPFRs. *Spectrum 3* - DMPO-O₂⁻ adduct formed in AcN media with 50 ug/ml EPFRs. *Spectrum 4* - DMPO-O₂⁻ adduct formed in AcN media with 25 ug/ml EPFRs. B) *Black line* – Expanded spectrum of DMPO-O₂⁻ adduct formed in AcN media with 50 ug/ml EPFRs (spectrum 3 in Fig. 4A); *Red line* - Expanded spectrum of DMPO-O₂⁻ formed in TiO₂ suspension in AcN media⁴⁰. * 200 mM DMPO+150 μM ferrous ammonium sulfate+2 mM H₂O₂ in DMSO (70%) / H₂O.



Figure 5. Hypothesized biological red-ox cycle of EPFRs originating from 2-MCP molecule adsorbed on a Cu(II)O domain. (ET – Electron Transfer) environmental PM largely exists as Fe(III), rather than Fe(II), and is not Fenton active.

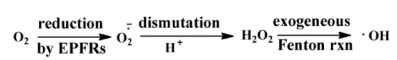
**Scheme 1.**

Table 1

Measured EPR Parameters of DMPO-OH Adduct in Water Solution as a Function of AcN Concentration

Measured EPR Parameters	% of AcN in Sample solution *		
	0	20	50
ΔH_{p-p} (G)	1.2	1.3	1.8
hfsc (G)	$\alpha_N = \alpha_H = 14.95$	$\alpha_N = \alpha_H = 14.60$	$\alpha_N = \alpha_H = 14.28$

* 50 μ g EPFRs'+150mM DMPO + AcN + buffer